The Journal of Immunology

The Role and Effects of Glucocorticoid-Induced Leucine Zipper in the Context of Inflammation Resolution

Juliana P. Vago, Luciana P. Tavares, Cristiana C. Garcia, Kátia M. Lima, Luiza O. Perucci, Érica L. Vieira, Camila R. C. Nogueira, Frederico M. Soriani, Joilson O. Martins, Patrícia M. R. Silva, Karina B. Gomes, Vanessa Pinho, Stefano Bruscoli, Carlo Riccardi, Elaine Beaulieu, Eric F. Morand, Mauro M. Teixeira and Lirlândia P. Sousa

J Immunol 2015; 194:4940-4950; Prepublished online 15 April 2015;
doi: 10.4049/jimmunol.1401722
http://www.jimmunol.org/content/194/10/4940

The Journal of Immunology is published twice each month by The American Association of Immunologists, Inc., 9650 Rockville Pike, Bethesda, MD 20814-3994.

Print ISSN: 0022-1767 Online ISSN: 1550-6606.

The Role and Effects of Glucocorticoid-Induced Leucine Zipper in the Context of Inflammation Resolution

Juliana P. Vago,*,†,‡ Luciana P. Tavares,*,† Cristiana C. Garcia,†,§ Kátia M. Lima,*,†,‡ Luiza O. Perucci,*,† Érica L. Vieira,† Camila R. C. Nogueira,*,† Frederico M. Soriani,¶ Joilson O. Martins,‖ Patrícia M. R. Silva,# Karina B. Gomes,* Vanessa Pinho,†,‡ Stefano Bruscoli, Carlo Riccardi,** Elaine Beaulieu,†† Eric F. Morand,†† Mauro M. Teixeira,† and Lirlândia P. Sousa*,†,‡**

Glucocorticoid (GC)-induced leucine zipper (GILZ) has been shown to mediate or mimic several actions of GC. This study assessed the role of GILZ in self-resolving and GC-induced resolution of neutrophilic inflammation induced by LPS in mice. GILZ expression was increased during the resolution phase of LPS-induced pleurisy, especially in macrophages with resolving phenotypes. Pretreating LPS-injected mice with *trans*-activator of transcription peptide (TAT)–GILZ, a cell-permeable GILZ fusion protein, shortened resolution intervals and improved resolution indices. Therapeutic administration of TAT-GILZ induced inflammation resolution, decreased cytokine levels, and promoted caspase-dependent neutrophil apoptosis. TAT-GILZ also modulated the activation of the survival-controlling proteins ERK1/2, NF-κB and Mcl-1. GILZ deficiency was associated with an early increase of annexin A1 (AnxA1) and did not modify the course of neutrophil influx induced by LPS. Dexamethasone treatment resolved inflammation and induced GILZ expression that was dependent on AnxA1. Dexamethasone-induced resolution was not altered in GILZ$^{-/-}$ mice due to compensatory expression and action of AnxA1. Our results show that therapeutic administration of GILZ efficiently induces a pro-apoptotic program that promotes resolution of neutrophilic inflammation induced by LPS. Alternatively, a lack of endogenous GILZ during the resolution of inflammation is compensated by AnxA1 overexpression. ***The Journal of Immunology*, 2015, 194: 4940–4950.**

Resolution of inflammation is an active and continuous process with production and activation of biochemical mediators and signaling pathways to ensure rapid and successful restoration of tissue homeostasis (1–3). During the resolution phase of inflammation, multiple proresolving molecules are produced to temper the inflammatory response and guarantee the return to homeostasis.

One of the most important endogenous proresolution pathways is that mediated by glucocorticoids (GCs) produced by the adrenal glands. Exploiting these physiological effects, GCs are among the most important drugs that have been developed for the treatment of inflammatory diseases. However, metabolic side effects of GCs limit their therapeutic application (4–6). The mechanisms of GCs are complex and depend on inhibition of transcription factors, such as NF-κB and AP-1, as well as induction of anti-inflammatory regulatory proteins such as annexin A1 (AnxA1), GC-induced leucine zipper (GILZ), and MAPK phosphatase (MKP)-1 (3). Thus, there is a growing interest in understanding the effects of GC-induced proteins that may allow dissociation of GC anti-inflammatory effects from their adverse metabolic effects.

GILZ was first identified in 1997 (7) and has been characterized as a novel GC-induced protein that mediates many anti-inflammatory effects of GC in leukocytes (5, 8). GILZ has been reported to interact with NF-κB and AP-1, and to inhibit the MEK/ERK1/2 pathway by binding to the upstream proteins Ras and Raf-1. These mechanisms are thought to be important for their ability to attenuate inflammation (8). GILZ appears to have a physiological role in the regulation of inflammatory mechanisms; however, there are few reports that explore its role in inflammatory disease (9–13).

AnxA1 is another GC-induced protein that has been shown to be anti-inflammatory and proresolving in various animal models of inflammation and in physiological conditions (4). Indeed, AnxA1

*Departamento de Análises Clínicas e Toxicológicas, Faculdade de Farmácia, Universidade Federal de Minas Gerais, Belo Horizonte, Minas Gerais 31270-901, Brazil; †Imunofarmacologia, Departamento de Bioquímica e Imunologia, Universidade Federal de Minas Gerais, Belo Horizonte, Minas Gerais 31270-901, Brazil; ‡Departamento de Morfologia, Universidade Federal de Minas Gerais, Belo Horizonte, Minas Gerais 31270-901, Brazil; §Laboratório de Vírus Respiratórios e do Sarampo, Instituto Oswaldo Cruz/FIOCRUZ, Rio de Janeiro 21040-360, Brazil; ¶Departamento de Biologia Geral, Instituto de Ciências Biológicas, Universidade Federal de Minas Gerais, Belo Horizonte, Minas Gerais 31270-901, Brazil; ‖Faculdade de Ciências Farmacêuticas, Universidade de São Paulo, São Paulo 05508-900, Brazil; #Laboratório de Inflamação, Instituto Oswaldo Cruz/FIOCRUZ, Rio de Janeiro 21040-360, Brazil; **Section of Pharmacology, Department of Medicine, University of Perugia, 06132 Perugia, Italy; and ††Monash University Centre for Inflammatory Diseases, Monash Medical Centre, Clayton, Victoria 3168, Australia

Received for publication July 11, 2014. Accepted for publication March 6, 2015.

This work was supported by grants from the Conselho Nacional de Desenvolvimento Científico e Tecnológico (Conselho Nacional de Pesquisas, Brazil), the Fundação de Amparo a Pesquisa do Estado de Minas Gerais (Brazil), the Pró-Reitoria de Pesquisa da Universidade Federal de Minas Gerais (Brazil) (Programa de Auxílio à Pesquisa de Doutores Recém-Contratados), National Health and Medical Research Council of Australia Grant 1011670, and by European Community's Seventh Framework Programme (FP7-2007-2013) Grant HEALTH-F4-2011-281608. K.B.G., P.M.R.S., V.P., M.M.T., and L.P.S. were supported by a Conselho Nacional de Pesquisas (Brazil) research productivity fellowships.

Address correspondence and reprint requests to Prof. Lirlândia P. Sousa or Prof. Mauro M. Teixeira, Departamento de Análises Clínicas e Toxicológicas, Faculdade de Farmácia, Universidade Federal de Minas Gerais, Avenida Antonio Carlos, 6627, Pampulha, Belo Horizonte, Minas Gerais 31270-901, Brasil (L.P.S.) or Departamento de Bioquímica e Imunologia, Instituto de Ciências Biológicas, Universidade Federal de Minas Gerais, Avenida Antonio Carlos, 6627, Pampulha, Belo Horizonte, Minas Gerais 31270-901, Brasil (M.M.T.). E-mail addresses: lipsousa72@gmail.com (L.P.S.) or mmtex@icb.ufmg.br (M.M.T.)

The online version of this article contains supplemental material.

Abbreviations used in this article: AnxA1, annexin A1; Dex, dexamethasone; GC, glucocorticoid; GILZ, glucocorticoid-induced leucine zipper; i.pl., intrapleural(ly); KO, knockout; MKP, MAPK phosphatase; Mres, resolution-promoting macrophage; TAT, *trans*-activator of transcription peptide; WT, wild-type.

www.jimmunol.org/cgi/doi/10.4049/jimmunol.1401722

limits initial steps of inflammation, specifically the recruitment of leukocytes and generation of proinflammatory mediators. AnxA1 also acts on the resolution phase of inflammation by inducing apoptosis of neutrophils (14, 15) and increasing efferocytosis by macrophages (16, 17). Importantly, AnxA1 production and activities are involved in proresolution effects of GCs (18) and histone deacetylase inhibitors (19). Recently, it was demonstrated in vitro that GILZ is a target of the anti-inflammatory effects of AnxA1 (20). However, whether AnxA1 cooperates with GILZ in vivo to convey the anti-inflammatory and proresolving activities of endogenous or synthetic GCs remains unknown.

In this study, we investigated the role of GILZ in natural and GC-driven resolution of inflammation. We demonstrate that GILZ is expressed during the resolving phase of inflammation in macrophages with proresolving phenotypes. Pharmacological treatment with recombinant GILZ protein reduces resolution intervals and promotes resolution of LPS-induced neutrophilic inflammation, whereas self-resolving inflammation was dependent on a compensatory balance between AnxA1 and GILZ expression.

Materials and Methods

Animals

All procedures described in this study had prior approval from the Animal Ethics Committee of Universidade Federal de Minas Gerais, Brazil (Comitê de Ética em Experimentação Animal/Universidade Federal de Minas Gerais protocol no. 15/2011). Male BALB/c mice (8–10 wk) bred in the Animal Facility of Centro de Bioterismo of Universidade Federal de Minas Gerais (Brazil) were housed under standard conditions and had free access to commercial chow and water. GILZ-deficient male mice were generated as described (13), and C57BL/6 littermates were bred in the animal facility of the Immunopharmacology Laboratory.

Drugs, reagents, and Abs

The peptide *trans*-activator of transcription peptide (TAT) and the TAT-GILZ fusion protein (constructed by inserting GILZ cDNA in the TAT-C vector to produce an in-frame fusion protein) were generated as described (9). Briefly, TAT and TAT-GILZ were in-frame cloned into the pGEX-4T2 plasmid (GE Healthcare). The pGEX-4T2 plasmid is a GST fusion vector carrying a tac promoter for chemically (isopropyl β-D-thiogalactopyranoside) inducible high-level expression of the protein. GST fusion protein was expressed in *Escherichia coli* grown at 30˚C and induced with 0.1 mM isopropyl β-D-thiogalactopyranoside for 90 min. Following lysis by sonication, most of the induced protein was found in the soluble material, which was purified with glutathione–Sepharose 4B beads (GE Healthcare) following the manufacturer's instructions. Eluted proteins were dialyzed for 48 h against PBS. Protein quantification and purity were evaluated by SDS-PAGE and by Coomassie blue staining. LPS contamination in each batch of TAT and TAT-GILZ was evaluated by using a *Limulus* amebocyte lysate chromogenic endotoxin quantification kit (Pierce, catalog no. 88282). LPS contamination was low (<0.5 endotoxin unit/ml or <0.05 ng). For comparison, the amount of LPS injected to induce cell recruitment was 1.250 endotoxin units (250 ng/cavity). ZVAD-fmk and Ac2-26 peptide were from Tocris Bioscience (Ellisville, MO). Rabbit anti–p-ERK1/2, anti–Mcl-1, and mouse anti–p-IκB-α Abs were from Cell Signaling Technology (Beverly, MA). Rabbit anti-GILZ and anti–MKP-1 and secondary anti-rabbit and anti-mouse peroxidase conjugate Abs were purchased from Santa Cruz Biotechnology (Santa Cruz, CA). Rabbit anti-AnxA1 was purchased from Invitrogen (Carlsbad, CA). Anti–β-actin, LPS (from *E. coli* serotype O:111:B4), and dexamethasone (Dex) were from Sigma-Aldrich (St. Louis, MO). Anti-AnxA1 antiserum was a gift from Dr. Steve Poole (Biotherapeutics Group, National Institute for Biological Standards and Control, U.K.).

Leukocyte migration into the pleural cavity induced by LPS

Mice received an intrapleural (i.pl.) administration of LPS (250 ng/cavity) or PBS as previously described (15, 21). Cells present in the pleural cavity were harvested at different times after LPS injection by washing the cavity with 2 ml PBS. Total cell counts were performed in a modified Neubauer chamber using Turk's stain. Differential cell counts were performed on cytocentrifuge preparations (Shandon III) stained with May–Grünwald–Giemsa using standard morphological criteria to identify cell types. The results are presented as the number of cells per cavity.

Treatment protocols

To evaluate the effect of anti-inflammatory/proresolving agents on LPS-induced pleurisy, mice were treated with the synthetic GC Dex (2.0 mg/kg, i.p.), Ac2-26 peptide (100 μg, i.p.), or TAT-GILZ peptide (0.2 mg/kg, i.p.) 4 h after LPS challenge. The peptide TAT (0.1 mg/kg, i.p.) was used as a control. In other experiments, TAT-GILZ or the control peptide were administered before LPS injection in a pretreatment protocol. To prevent the action of AnxA1 induced by Dex, mice were treated with anti-AnxA1 antiserum (0.1 ml hyperimmune serum diluted in 100 μl PBS/mouse, i.p.) (22). Nonimmune goat serum was used as control. ZVAD-fmk (1 mg/kg), a broad-spectrum caspase inhibitor (21), was given systemically (i.p.) 15 min before TAT-GILZ injection. Drugs were dissolved in DMSO or ethanol and diluted further in PBS. Control mice received vehicle only.

Calculation of resolution indices

We quantified the resolution indices as described (23, 24). Murine pleural exudates were collected at 4, 8, 24, 48, and 72 time points after challenge. The numbers of PMN and mononuclear cells were determined by total and differential leukocyte counting. Using these two cell types, the resolution of acute inflammation was defined in quantitative terms by the following resolution indices: 1) magnitude (ψ_{max} and T_{max}), where ψ_{max} indicates maximal PMN and T_{max} indicates time point when PMN numbers reach maximum; 2) duration (T_{50}), which indicates time point when PMN numbers reduce to 50% of maximum; and 3) resolution interval (R_i), which indicates interval between T_{max} and T_{50}, when 50% PMN are lost from the pleural cavity.

Assessment of leukocyte apoptosis

Apoptosis was assessed morphologically as previously reported (15, 21). Briefly, cells (5×10^4) collected after LPS administration were cytocentrifuged, fixed and stained with May–Grünwald–Giemsa, and counted using oil immersion microscopy (×100 objective) to determine the proportion of cells with distinctive apoptotic morphology (cells with chromatin condensation, nuclear fragmentation, and formation of apoptotic bodies out or inside macrophages). At least 500 cells were counted per slide, and results are expressed as the mean ± SEM of percentage of cells with apoptotic morphology. Assessment of apoptosis was also performed by flow cytometry using FITC-labeled annexin V (ApoDETECT Annexin V^{FITC} kit, Invitrogen) and propidium iodide, as an index of loss of nuclear membrane integrity.

Flow cytometry analysis for leukocyte populations and expression of GILZ and AnxA1

Cells present in the pleural cavity were harvested at 24 and 48 h after administration of LPS or PBS (24 h). The populations of macrophages and neutrophils were analyzed by staining with fluorescent mAbs against F4/80 (PE-Cy7, eBioscience, San Diego, CA), Gr1 (FITC, BioLegend, San Diego, CA), Gr1 (PE, BioLegend), CD11b (PE-Cy5, BD Biosciences, San Jose, CA), CD11c (PE-Cy7, BD Biosciences), GILZ (PE, eBioscience), AnxA1 (Santa Cruz Biotechnology, Santa Cruz, CA), and anti-rabbit (Alexa 647, BD Biosciences). After being stained for surface markers, cells were permeabilized with permeabilization buffer (eBioscience) for 30 min. Stained cells were acquired in a BD LSRFortessa cell analyzer (BD Biosciences) and analyzed using FlowJo software (Tree Star, Ashland, OR). Gating strategy is ilustrated in Supplemental Fig. 2D. Macrophage populations were defined according to F4/80, Gr1, and CD11b expression. Cells selected in the side scatter/forward scatter gate (*first dot plot* in Supplemental Fig. 2D) were analyzed for F4/80 and Gr1 expression (*second dot plot* in Supplemental Fig. 2D). $F4/80^+$ cells were further analyzed for intensity of F4/80 expression (*first row* in Supplemental Fig. 2D); the $F4/80^{med}$ population was then evaluated for CD11b expression, then $F4/80^{med}CD11b^{low}$ cells, considered resolution-promoting macrophages (Mres). The $F4/80^+Gr1^-$ population was further analyzed for intensity of F4/80 expression (*second row* in Supplemental Fig. 2D); the $F4/80^{high}$ population was then evaluated for CD11b expression; the M2 population is $F4/80^{high}$, $Gr1^-$, $CD11b^{high}$. The $F4/80^+Gr1^+$ population was further analyzed for intensity of F4/80 expression (*third row* in Supplemental Fig. 2D); the $F4/80^{low}$ population was then evaluated for CD11b expression; the M1 population is then $F4/80^{low}$, $Gr1^+$, $CD11b^{med}$. The three macrophages populations were evaluated for GILZ and AnxA1 expression (*fifth* and *sixth columns* in Supplemental Fig. 2D). The percentage presented in each dot plot is related to the previous population analyzed. AnxA1 labeling was performed at 1:500 dilution, and cells from AnxA1-deficient mice showed no detectable labeling (not shown). Negative controls were cells stained with fluorochrome-bound secondary Abs only.

Quantitation of mRNA expression by real-time PCR

Total RNA from cells harvested from the pleural cavity was extracted using the RNeasy Mini kit (Qiagen, Crawley, U.K.) according to the manufacturer's instructions. cDNA was synthetized using 1 μg RNA with SuperScript III reverse transcriptase (Invitrogen), following the manufacturer's instructions. Real-time PCR was performed in duplicate, with 1 μl cDNA at a concentration of 100 ng, 0.5 μM primers and Power SYBR Green PCR Master Mix (Applied Biosystems, Warrington, U.K.) using StepOne (Applied Biosystems, Foster City, CA, USA). The data were analyzed using StepOne System software with a cycle threshold (Ct) in the linear range of amplification and then processed by the $2^{-\Delta\Delta Ct}$ method. Primers (Integrated DNA Technologies) used are the following: *AnxA1* (5′-ATCAGCGGTGAGCCCCTATC-3′, 5′-TTCATCCAGGGGGCTTTCCT-G-3′), *GILZ* (5′-CAGCAGCCACTCAAACCAGC-3′, 5′-ACCACATCCCC-TCCAAGCAG-3′), and *Gapdh* (5′-AGAAGACTGTGGATGGCCCC-3′, 5′-TGACCTTGCCCACAGCCTT-3′). A dissociation step was always included to confirm the absence of unspecific products. In each experiment, samples of all groups were run on one plate with two technical replicates. *Gapdh* was used as an endogenous control to normalize the variability in expression levels, and results were expressed as fold increase.

Lysate preparation and Western blot analysis

Inflammatory cells harvested from the pleural cavity were washed with PBS and whole-cell extracts were prepared as previously described (15, 25). Protein amounts were quantified with the Bradford assay reagent from Bio-Rad (Bio-Rad, Hercules, CA). Extracts (50 μg) were separated by electrophoresis on a denaturing 10–15% polyacrylamide-SDS gel and electrotransferred to nitrocellulose membranes, as described (26). Membranes were blocked overnight at 4°C with PBS containing 5% (w/v) nonfat dry milk and 0.1% Tween 20, washed three times with PBS containing 0.1% Tween 20, and then incubated with specific primary Abs (Mcl-1, p-ERK1/2, p–IκB-α, AnxA1, GILZ, MKP-1, or anti β-actin) using a dilution of 1:1000 in PBS containing 5% (w/v) BSA and 0.1% Tween 20. After washing, membranes were incubated with appropriated HRP-conjugated secondary Ab (1:3000). Immunoreactive bands were visualized by using ECL detection system, as described by the manufacturer (GE Healthcare, Piscataway, NJ).

Measurement of cytokines and chemokines

The levels of cytokines IL-1β, TNF-α, and IL-6 and of the chemokines CCL2 and CCL5 were measured in supernatants obtained from pleural cavity washes after TAT-GILZ treatment or at different time points after LPS challenge in GILZ-deficient male mice and C57BL/6 littermates by ELISA, using commercially available Abs according to the procedures supplied by the manufacturer (R&D Systems, Minneapolis, MN).

Corticosterone assay

Blood samples of mice injected with saline or LPS were collected with heparin and centrifuged at 2000 × *g* for 15 min for plasma collection. Samples were stored at −80°C until assayed. Corticosterone was measured using a corticosterone EIA kit (Cayman Chemical, Ann Arbor, MI), according to the manufacturer's instructions.

Statistical analysis

All results are presented as the means ± SEM. Data were analyzed by one-way ANOVA, and differences between groups were assessed using the Student–Newman–Keuls posttest. When only two groups were evaluated, a Student *t* test was used. A p value <0.05 was considered significant. Calculations were performed using the Prism 5.0 software for Windows (GraphPad Software, San Diego, CA).

Results

Self-resolving inflammation of LPS-induced pleurisy is accompanied by increased expression of GILZ in resolution macrophages

We performed experiments in a well-established model of LPS-induced pleurisy (15, 21). In this model i.pl. injection of LPS induces a time-dependent influx of neutrophils into the pleural cavity of mice that peaks at 8–24 h and decreases thereafter. Resolution of neutrophilic inflammation took place at 48 h, coincident with the mononuclear cell influx into the pleural cavity (Fig. 1A). Next, we investigated whether GILZ expression was associated with resolution phase of neutrophilic inflammation and whether macrophages were a source of this protein. As observed in Western blot (Fig. 1B) and quantitative PCR analysis (Fig. 1C), GILZ was detected in PBS-injected mice, virtually disappeared during LPS-induced neutrophilic infiltration, and was again strongly detected during the resolution phase (48–72 h). The kinetics of AnxA1 expression were quite similar to GILZ as shown by Western blot (15) and quantitative PCR (Supplemental Fig. 1). In the early phase of inflammation macrophages are an important source of cytokines and inflammatory mediators, but at later time points this cell type is crucial for the resolution of inflammatory response (27). Based on a recent description of three macrophage populations, that is, M1 ($F4/80^{low}Gr1^{+}Cd11b^{med}$), M2 ($F4/80^{high}Gr1^{-}Cd11b^{high}$), and Mres ($F4/80^{med}Cd11b^{low}$) (28, 29), we performed evaluation of these populations by flow cytometry in cells from the pleural cavity of LPS-injected mice. As shown in Fig. 1D and 1G, we detected more M2 and Mres macrophages at 48 h. M2 macrophages were detected in PBS-injected mice, were significantly reduced at 8 h, and significantly increased at 48 h after LPS challenge (Fig. 1D). The number of M2 cells was higher than that of Mres (Fig. 1D, 1G). The kinetics of M2 macrophage numbers were quite similar to those of GILZ and AnxA1 expression. In contrast, M1 macrophages were not detected in PBS-injected mice, were abundant at 8 h, and virtually disappeared 48 h after LPS challenge (Supplemental Fig. 2A). In M1 macrophages, GILZ expression was not detected in PBS-injected mice, but it was increased at 8 and 48 h after LPS injection (Supplemental Fig. 2B). In contrast, AnxA1 expression in M1 macrophages was increased at 8 h but virtually disappeared 48 h after LPS challenge (Supplemental Fig. 2C). Significantly, expression of both GILZ and AnxA1 was increased in M2 (Fig. 1E and 1F, respectively) and Mres macrophages (Fig. 1H and 1I, respectively) at 48 h; $AnxA1^{+}$ Mres macrophages were approximately 10-fold more abundant than $GILZ^{+}$ Mres macrophages (Fig. 1H, 1I). The gating strategy used is shown in Supplemental Fig. 2D. These results indicate that changes in GILZ expression in macrophages coincide with self-resolving neutrophilic inflammation.

Pre- and posttreatment of LPS-inflamed mice with the TAT-GILZ peptide induces resolution of neutrophilic inflammation

Next, we evaluated the effects of TAT-GILZ, a GILZ fusion protein containing a TAT peptide to allow the in vivo delivery of the protein, on resolution of inflammation. TAT-GILZ or the peptide control (TAT peptide only) were injected before LPS challenge, and cells were collected at 4, 8, 24, 48, and 72 h after challenge. We quantified the resolution interval (Ri) by defining acute inflammatory parameters (23, 24). Pretreatment with TAT-GILZ significantly reduced the number of PMN recruited to the pleural cavity and shortened R_i by ∼12 h (Fig. 2A). To verify its therapeutic potential, TAT-GILZ was administered 4 h after LPS challenge and cells were obtained from the pleural cavity by washing at 5, 8, and 24 h after LPS administration. Posttreatment of mice with TAT-GILZ greatly decreased neutrophil accumulation in the pleural cavity at 8 and 24 h (Fig. 2C). In both protocols, TAT-GILZ treatment did not significantly alter the number of mononuclear cells (Fig. 2B, 2D), and TAT peptide alone had no significant effect. In keeping with these findings, treatment of mice with TAT-GILZ 4 h after LPS challenge decreased pleural IL-6 and TNF-α levels (Fig. 2E and 2F, respectively) but did not modify pleural IL-1β levels (Fig. 2G). These results indicate that pharmacological treatment with a GILZ fusion protein induces resolution of neutrophilic inflammation.

TAT-GILZ promotes resolution of neutrophilic inflammation by inducing neutrophil apoptosis and inhibiting survival pathways

We queried whether the induction of leukocyte apoptosis was an underlying mechanism of TAT-GILZ–induced resolution of LPS-

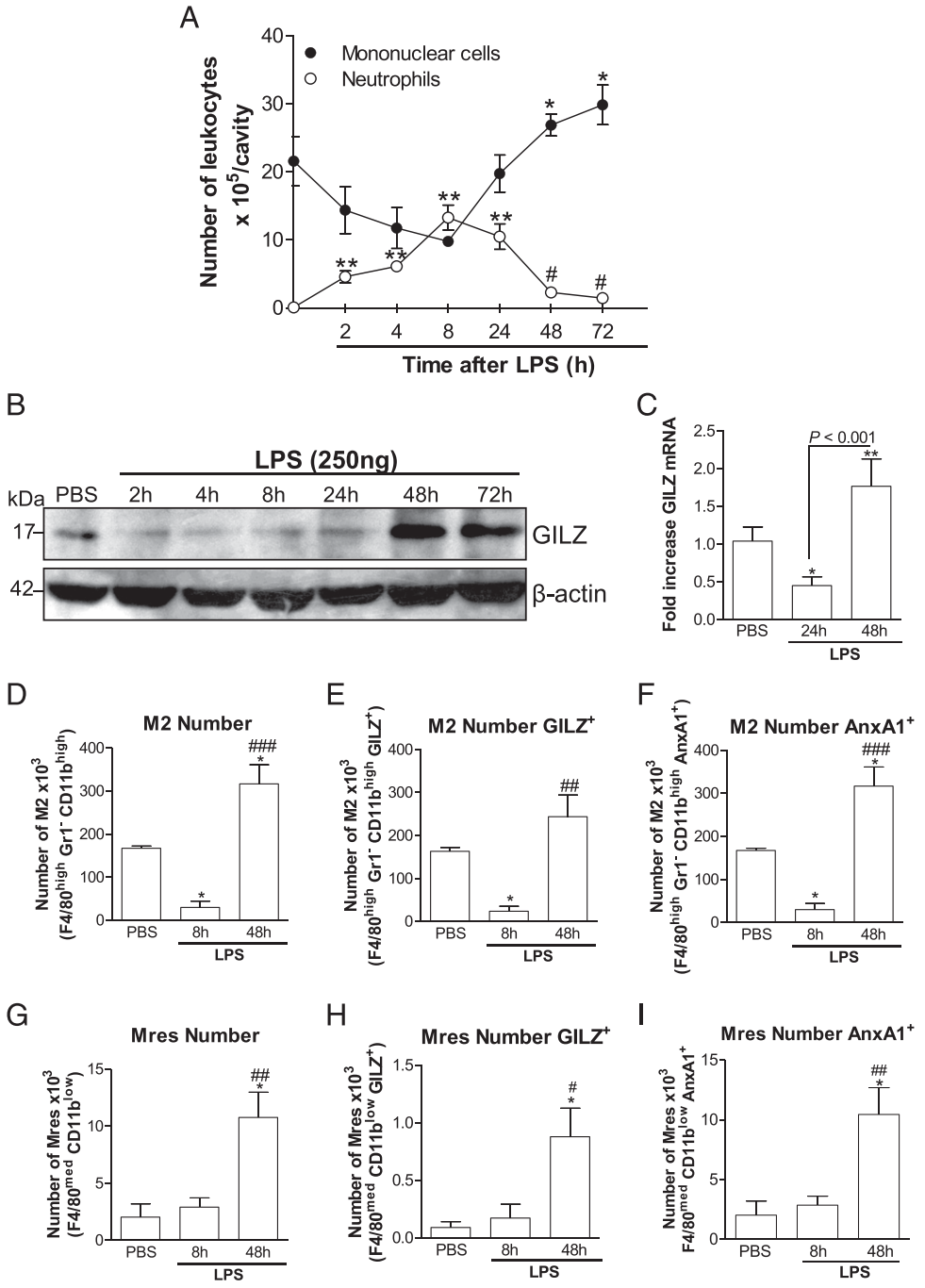

FIGURE 1. Time course of GILZ expression during LPS-induced pleurisy. Mice were injected with LPS (250 ng/cavity, i.pl.) or PBS and the cells present in the pleural cavity were harvested at several time points and processed for total and differential leukocyte counts of cytospin preparations by (**A**) light microscopy, (**B**) Western blot, and (**C**) quantitative PCR analysis for GILZ expression. Flow cytometry analysis of pleural leukocytes collected after PBS or LPS injection is shown. (**D**) M2 ($F4/80^{high}Gr1^{-}CD11b^{high}$) number, (**E**) M2 expressing GILZ, and (**F**) AnxA1. (**G**) Mres ($F4/80^{med}CD11b^{low}$) number, (**H**) Mres expressing GILZ, and (**I**) AnxA1. Results are expressed as the number of cells per cavity or fold increase and are shown as the mean ± SEM of at least five mice in each group. Quantitative PCR data were performed in samples from control and treated groups of at least five animals for each time point. Analyses of gene expression were performed with two technical replicates with samples of all groups run on one plate. For loading control, membranes were reprobed with anti–β-actin. Blots are representative of three independent experiments using pooled cells from at least five animals in each experiment. $^{*}p < 0.05$, $^{**}p < 0.01$ when compared with PBS-injected mice. $^{\#}p < 0.05$, $^{\#\#}p < 0.01$, $^{\#\#\#}p < 0.001$ when compared with 8 h after LPS-injected mice.

induced pleurisy. To investigate this, TAT-GILZ–injected mice were pretreated with a broad-spectrum caspase inhibitor, zVAD-fmk. The results presented in the Fig. 3A show that the effect of TAT-GILZ on pleural neutrophil numbers was prevented by the pan-caspase inhibitor. Importantly, treatment with zVAD alone did not alter the kinetics of neutrophil recruitment after injection of LPS (21). Accordingly, treatment of mice with TAT-GILZ induced neutrophil apoptosis in the pleural cavity, as assessed using either morphological criteria (Fig. 3B) or annexin V staining (Fig. 3C). In contrast, treatment with TAT-GILZ did not induce apoptosis of macrophages (Supplemental Fig. 3). We also evaluated biochemical markers of survival pathways that control neutrophil lifespan. Using Western blotting of cell extracts of TAT-GILZ–treated mice, we found that treatment with TAT-GILZ reduced

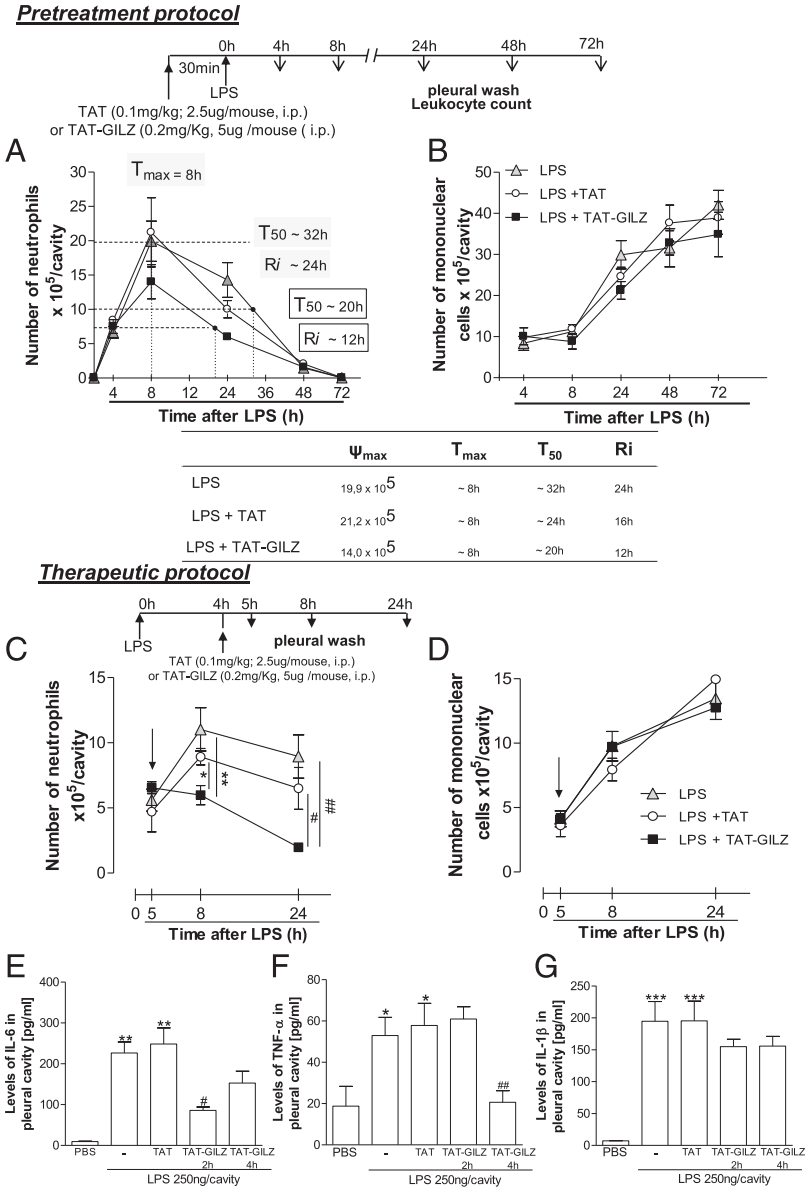

FIGURE 2. Effect of pre- and posttreatment of mice with TAT-GILZ peptide on LPS-induced pleurisy. For pretreatment, mice received an injection of TAT (0.1 mg/kg, i.p.), TAT-GILZ (0.2 mg/kg, i.p.), or vehicle. After 15 min, mice were challenge with LPS (250 ng/cavity, i.pl.). For posttreatment, mice were injected with LPS (250 ng/cavity, i.pl.) and 4 h later received an injection of TAT or TAT-GILZ. (**A** and **C**) The number of neutrophils and (**B** and **D**) mononuclear cells were evaluated at several time points. Of note, T_{max} = 8 h, the time point when PMN numbers reach maximum; $T_{50} \sim 20$ h, the time point when PMN numbers reduce to 50% of maximum; and $R_i \sim 12$ h, resolution interval, the time period when 50% PMN are lost from the pleural cavity. Levels of (**E**) IL-6, (**F**) TNF-α, and (**G**) IL-1β were measured by ELISA in supernatants obtained from pleural cavity washes after 2 and 4 h of TAT or TAT-GILZ treatment of 4 h LPS-injected mice. Results are expressed as the number of cells per cavity or pleural cytokines levels (in pg/ml) and are shown as the mean ± SEM of at least five mice in each group. $^{*}p < 0.05$, $^{**}p < 0.01$, $^{***}p < 0.001$ when compared with PBS-injected mice. $^{\#}p < 0.05$, $^{\#\#}p < 0.01$ when compared with TAT only or 8 h after LPS-challenged mice.

cellular levels of p-ERK1/2, p–IκB-α, and Mcl-1 (Fig. 3D). Taken together, these findings indicate that GILZ plays an important role in the signaling events leading to the neutrophil proapoptotic program during the resolution of acute inflammation.

Resolution of neutrophilic inflammation in GILZ$^{-/-}$ mice was accompanied by increased levels of AnxA1 and corticosterone

In attempt to characterize better the role of endogenous GILZ in resolution of acute inflammation, we conducted a kinetic study of LPS-induced pleurisy in GILZ$^{-/-}$ mice and compared them to wild-type (WT) littermates (C57BL/6). The resolution of inflammation was accompanied by decreased neutrophil accumulation in the pleural cavity in both GILZ$^{-/-}$ and WT mice (Fig. 4A). The number of pleural mononuclear cells at 48 h after LPS was lower in GILZ$^{-/-}$ mice than in WT mice (Fig. 4B). Pleural levels of the cytokines IL-6 and TNF-α and monocyte chemoattractive chemokines CCL2 and CCL5 were similar in WT and GILZ$^{-/-}$ mice (Fig. 4C).

Based on previous studies in which using small interfering RNA strategies to inhibit GILZ resulted in exacerbation of inflammatory response (10, 13), similar resolution of LPS-induced inflammation in GILZ$^{-/-}$ and WT mice (Fig. 4A) was unexpected. We hypothesized the existence of compensatory mechanisms such as the expression of other GC-induced proteins in the setting of GILZ deficiency. Interestingly, GILZ$^{-/-}$ mice showed an early increase of the active intact anti-inflammatory 37-kDa form of AnxA1, but not MKP-1, another GC-induced anti-inflammatory protein that inhibits MAPK activation (Fig. 4D). GILZ$^{-/-}$ mice had increased expression of AnxA1 without stimulation (PBS injected mice) as compared with WT mice (Supplemental Fig. 4). When mice were challenged with LPS, detectable AnxA1 was almost entirely in the cleaved (inactive) form in WT mice, whereas intact AnxA1 remained abundant in GILZ$^{-/-}$ mice and AnxA1 mRNA was increased (Supplemental Fig. 4).

It has been demonstrated that lack of AnxA1 results in increased numbers of corticotrophs (30), and AnxA1$^{-/-}$ mice show increased corticosterone levels after inflammatory stimulus (31). Therefore, we hypothesized that an increase in corticosterone levels could underlie the increased expression of AnxA1 in GILZ-deficient mice. Plasma corticosterone levels in GILZ$^{-/-}$ mice after LPS stimulation were twice those observed in WT mice (WT, 60.7 ± 11.9 ng/ml; GILZ$^{-/-}$, 126.5 ± 30.6 ng/ml; $p < 0.05$).

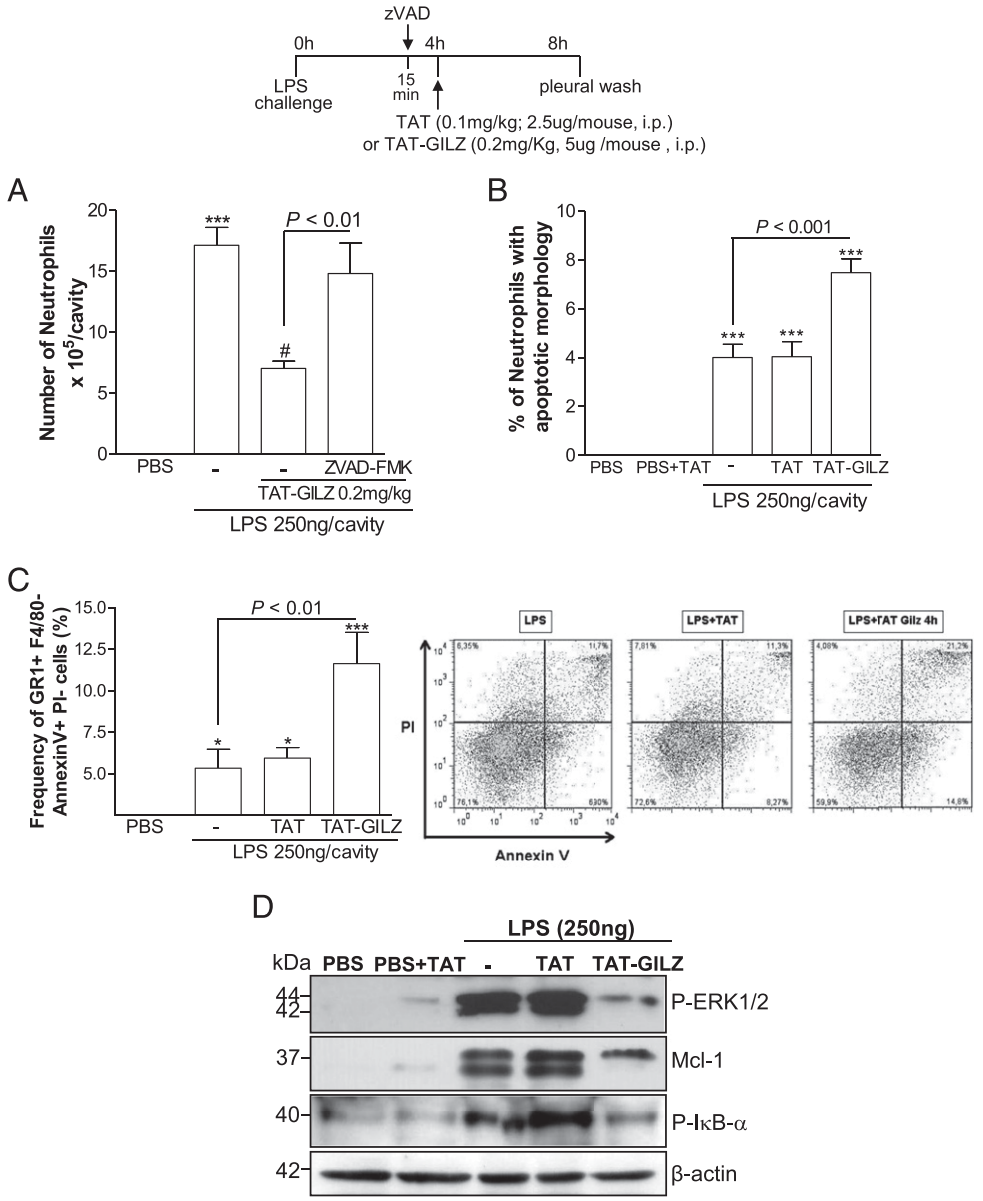

FIGURE 3. Effect of treatment with TAT-GILZ on neutrophil apoptosis in vivo. Mice were injected with LPS (250 ng/cavity, i.pl.) or PBS and 4 h later received an injection of TAT (0.1 mg/kg, i.p.), TAT-GILZ (0.2 mg/kg, i.p.), or vehicle. The pan-caspase inhibitor zVAD-fmk (1 mg/kg, i.p.) was given 15 min before the peptide. (**A**) The number of neutrophils, (**B**) cells with distinctive apoptotic morphology, (**C**) frequency of annexin V^+ neutrophils, and (**D**) Western blot to detection of p-ERK, Mcl-1, and p–IκB-α were evaluated 4 h after peptide treatment. For loading control, membranes were reprobed with anti–β-actin. Blots are representative of three independent experiments using pooled cells from at least five animals in each experiment. $^*p < 0.05$, $^{***}p < 0.001$ when compared with PBS-injected mice. $^{\#}p < 0.05$ when compared with 8 h after LPS-challenged mice.

These data are akin to those observed when comparing AnxA1-deficient mice (31), suggesting a regulatory effect on corticosterone production in absence of either of these GC-induced proteins. Taken together, these findings suggest that self-resolution of inflammation in $GILZ^{-/-}$ mice may depend on a compensatory effect mediated by overexpression of AnxA1 induced by endogenous GC.

Anti-AnxA1 abolished Dex-induced GILZ accumulation

AnxA1 is a GC-induced protein that mediates the anti-inflammatory and proresolving activities of endogenous and exogenous GC (15, 18, 32). It was demonstrated in in vitro experiments using $AnxA1^{-/-}$ macrophages that GILZ is a mediator of the anti-inflammatory effects of AnxA1 (20). Therefore, we asked whether AnxA1 is upstream of GILZ during responses to exogenous GC in our in vivo phlogistic settings. Treatment of LPS-injected mice with Dex decreased pleural neutrophil accumulation (Fig. 5A). Compared to PBS-treated controls, the administration of LPS markedly inhibited GILZ expression in pleural cells, but this effect was reversed by GC treatment, as evidenced by increased GILZ expression in Dex-treated mice (Fig. 5B). To evaluate whether AnxA1 could control GILZ expression in vivo, mice were treated with anti-AnxA1 neutralizing Ab before Dex treatment. Neutralization of AnxA1 abolished the effects of Dex on neutrophil accumulation (Fig. 6C) as previously shown (15) and inhibited the expression of GILZ (Fig. 5C), suggesting that AnxA1 is required for GC induction of GILZ in vivo. Next, we evaluated whether Ac2-26, a synthetic peptide that contains the N-terminal active portion of AnxA1, could induce GILZ expression. By flow cytometry, we found that Ac2-26 peptide treatment increased intracellular GILZ in macrophages ($F4/80^+$ cells) within 1 h (Fig. 5D). This result was not seen in neutrophils, examined by

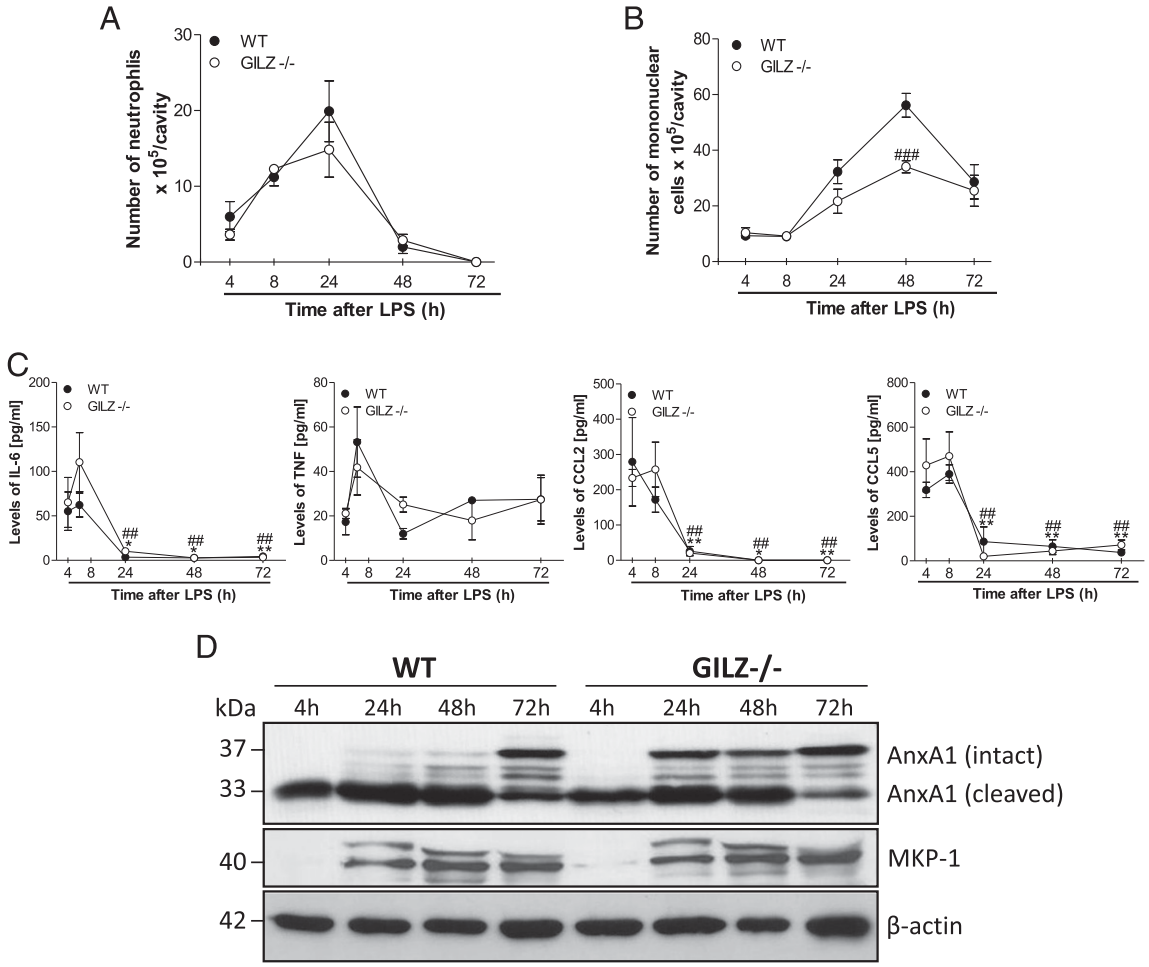

FIGURE 4. Time course of leukocyte influx, cytokine/chemokine, and AnxA1 levels during LPS-induced inflammation in WT and GILZ $^{-/-}$ mice. WT and GILZ$^{-/-}$ mice were injected with LPS (250 ng/cavity, i.pl.) and the cells present in the pleural cavity were harvested at different times and processed for total and differential leukocyte counts of cytospin preparations by (**A** and **B**) light microscopy and (**D**) Western blot analysis for AnxA1 and MKP-1. (**C**) Levels of IL-6, TNF-α, CCL2, and CCL5 (in pg/ml) were measured by ELISA assay in supernatants obtained from pleural cavity washes after LPS injection. Results are shown as the mean ± SEM of at least four mice in each group. For loading control, membranes were reprobed with anti–β-actin. Blots are representative of two independent experiments using pooled cells from at least four animals in each experiment. $^{###}p < 0.01$ when GILZ KO mice were compared with WT mice 48 h after LPS challenge. For levels of IL-6, TNF-α, CCL2, and CCL5: $*p < 0.05$, $**p < 0.01$ when compared with 8 h after LPS-challenged mice WT groups. $^{##}p < 0.01$ when compared with 4 or 8 h after LPS-challenged mice KO groups.

labeling GILZ in cells stained with Gr1$^+$ in the same experimental setting (data not shown).

Neutralizing AnxA1 in GILZ$^{-/-}$ mice abolishes resolution of neutrophilic inflammation

Next, we queried whether GC could induce resolution of inflammation in the absence of GILZ. Treatment of LPS-injected mice with Dex promoted resolution of neutrophilic inflammation in both WT and GILZ$^{-/-}$ mice genotypes (Fig. 6A). In WT mice, resolution of inflammation was associated with increased expression of intact AnxA1. As shown before (Fig. 4D, Supplemental Fig. 4A), GILZ$^{-/-}$ mice expressed increased intact AnxA1 in pleural cavity cells after LPS injection (compare *lanes 1* and *3*, Fig. 6B), and this was not further increased by Dex treatment (compare *lanes 3* and *4*, Fig. 6B). Finally, we investigated whether inhibiting AnxA1 in GILZ$^{-/-}$ mice could affect the phenotype of these mice. By using an AnxA1 neutralizing Ab previously used in other studies (15, 22), we showed that mice in which AnxA1 was neutralized were refractory to resolution induced by Dex (Fig. 6C), indicating that by preventing the compensatory effects of AnxA1, GILZ$^{-/-}$ mice lost the ability to resolve inflammation in response to GC treatment. Of note, treatment of mice with a control goat nonimmune serum had no effect on the resolution of inflammation (data not shown). These results clearly suggest that enhanced AnxA1 expression compensates for the lack of GILZ in mediating acute and GC-induced resolution of inflammation.

Discussion

GCs are potent anti-inflammatory and immunosuppressive drugs that are used therapeutically for the treatment of many inflammatory conditions. The broad-spectrum effects of GCs depend on their inhibitory effects on transcription factors, such as NF-κB and AP-1, and their capacity to induce anti-inflammatory regulatory proteins. Our group has recently shown the importance of AnxA1, a GC-induced protein, in driving natural and Dex-induced resolution of inflammation (15). Another GC-induced protein, GILZ, has been reported to interact with the same transcription factors as those of the GC receptor, and thereby to inhibit inflammation (8). However, the role of endogenous GILZ on natural and GC-induced resolution of acute inflammation has not been established. In this work, we studied whether GILZ mediates GC effects in the resolution of inflammation and investigated the proresolving properties of exogenously administrated GILZ. Moreover, because GILZ mediates AnxA1 anti-inflammatory ac-

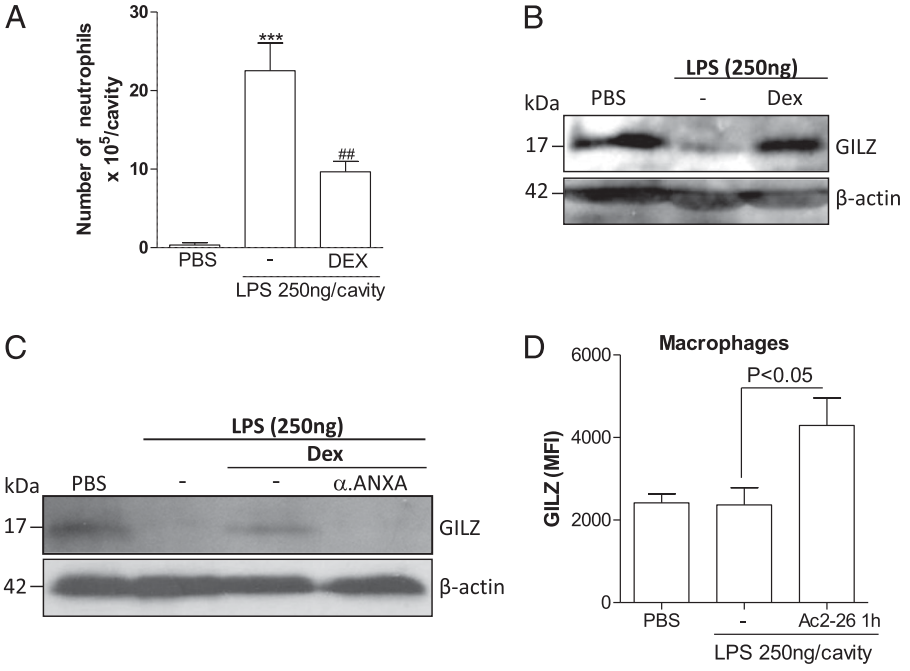

FIGURE 5. Effect of treatment with anti-AnxA1 antiserum on Dex-induced resolution of acute inflammation. Mice were injected with LPS (250 ng/cavity, i.pl.) or PBS and 4 h later received an injection of Dex (2 mg/kg, i.p.) or Ac2-26 (100 μg/cavity, i.pl.). Cells present in the pleural cavity were harvested 4 h after Dex or 1 h after Ac2-26 treatment. (**A**) Neutrophil counts and (**B** and **C**) Western blot for GILZ detection 4 h after Dex treatment. (**D**) Mean fluorescence intensity (MFI) of intracellular GILZ, evaluated by flow cytometry, in macrophages ($F4/80^+$ cells) 1 h after Ac2-26 treatment. Results are shown as the mean ± SEM of at least five mice in each group. For loading control, membranes were reprobed with anti–β-actin. Blots are representative of three independent experiments using pooled cells from at least five animals in each experiment. $^{***}p < 0.001$ when compared with PBS-injected mice, $^{\#\#}p < 0.01$ when compared with 8 h after LPS-challenged mice.

tivity in macrophages (20), we investigated the possible relationship between GILZ and AnxA1 in the resolution of neutrophilic inflammation. We found that GILZ is expressed in resolving Mres and M2 macrophages, suggesting that GILZ could play a key role in macrophage-induced resolution activities. Exogenous administration of a GILZ fusion protein (TAT-GILZ) promoted resolution of acute inflammation by inducing neutrophil apoptosis. In $GILZ^{-/-}$ mice, despite decreased mononuclear cell numbers, natural resolution of inflammation was unaltered, associated with enhanced plasma levels of corticosterone and early appearance of intact AnxA1. These latter results suggest that AnxA1 compensates for the lack of GILZ and permits natural resolution of inflammation in $GILZ^{-/-}$ mice. Finally, we showed that GILZ expression is dependent on AnxA1 during Dex-induced resolution of LPS inflammation, and Dex-induced resolution of inflammation is preserved in $GILZ^{-/-}$ mice, an effect explained by a compensatory increase in expression of AnxA1.

The kinetics of GILZ expression during a self-resolving model of pleurisy were similar to kinetics of AnxA1 expression (and as described in Ref. 15); that is, resident cells of the pleural cavity express GILZ and during the productive phase of LPS-induced pleurisy GILZ expression is inhibited. Indeed, it has been demonstrated that GILZ is downregulated in human alveolar macrophages upon TLR activation (33) and in HUVECs and macrophages upon treatment with TNF-α (34). In contrast, during the resolution phase, 48–72 h after LPS, GILZ expression was upregulated, and cells producing GILZ and AnxA1 were mostly Mres and M2 macrophages.

Macrophages are thought to be important at the onset of inflammation by producing proinflammatory mediators and performing effector functions. As the inflammatory response evolves, macrophages are reprogrammed toward a more resolving/restorative phenotype and are orchestrators of a series of events leading to successful resolution of inflammation (27, 35). One of the main functions of macrophages is elimination of apoptotic granulocytes (efferocytosis). Indeed, efferocytosis itself may reprogram macrophages with change of their phenotype. In models of self-resolving inflammation, various phenotypes of macrophages may coexist (28, 36, 37). M2 (or M2-like) macrophages are highly efferocytic and produce anti-inflammatory molecules such as IL-10 and TGF-β and biologically active amounts of proresolving mediators, including resolvins, protectins, and maresins (29, 38). Such mediators have the potential to inhibit further PMN recruitment, intensify monocyte migration, and amplify efferocytosis. M2 macrophages then switch to Mres phenotype, which display reduced phagocytosis, but instead produce antifibrotic and antioxidant proteins that limit tissue damage

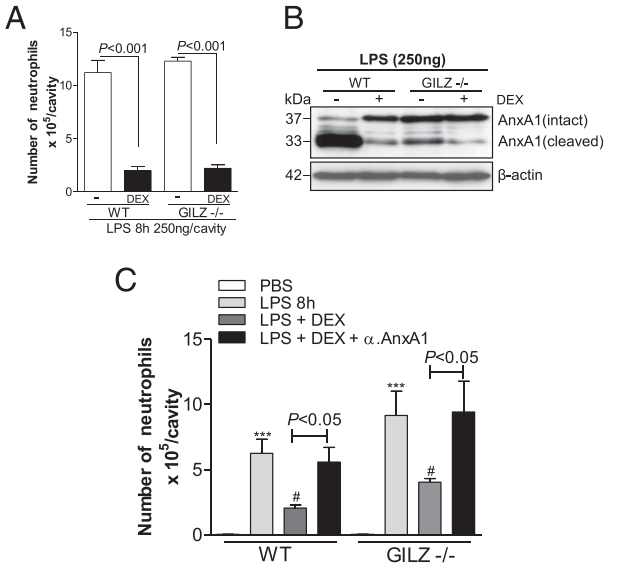

FIGURE 6. Effect of treatment with Dex and anti-AnxA1 antiserum in $GILZ^{-/-}$ mice. WT and $GILZ^{-/-}$ mice were injected with LPS (250 ng/cavity, i.pl.) or PBS and 4 h later received an injection of Dex (2 mg/kg, i.p.) or antiserum anti-AnxA1 (200 μl, i.p.) 1 h before Dex. Cells present in the pleural cavity were harvested 4 h after Dex or Dex plus anti-AnxA1 and processed for (**A** and **C**) neutrophil counts and (**B**) Western blot analysis of AnxA1. Results are shown as the mean ± SEM of at least five mice in each group. For loading control, membranes were reprobed with anti–β-actin. Blots are representative of two independent experiments using pooled cells from at least five animals in each experiment. $^{***}p < 0.001$ when compared with PBS-injected mice, $^{\#}p < 0.05$ when compared with 8 h after LPS-challenged mice.

and fibrosis (28). It has been demonstrated that GILZ is constitutively expressed in nonphlogistic conditions in human and murine macrophages (39). In the present study, we demonstrated that GILZ was expressed in M2 and Mres macrophages and its appearance coincides with resolution of inflammation. Indeed, GILZ acts physiologically to balance the inflammatory process (5), and in this study we show, to our knowledge for the first time, a temporal relationship between increases in GILZ and M2/Mres macrophages during the resolution of inflammation. Many mediators can accelerate the clearance of apoptotic granulocytes mediated by macrophages, including AnxA1, IL-10, and proresolution lipids (2). The increased expression of GILZ and AnxA1 (15) observed during the resolution phase of inflammation may contribute to increase the efferocytic capacity of macrophages, an effect already demonstrated for AnxA1 (17, 40).

Similar to AnxA1, GILZ has been shown to mediate several anti-inflammatory effects of GC, including modulation of T lymphocyte activation, apoptosis of thymocytes, and antiproliferative and anti-inflammatory activities, and it is upregulated by IL-10 and TGF-β in several cell types (7, 8). More recently, a study showed that GILZ promoted the induction of regulatory T cells and that lack of GILZ in T cells of GILZ knockout (KO) mice caused the development of spontaneous colitis (41). In this study, we demonstrated that treating mice with a TAT-GILZ fusion protein induced resolution of neutrophilic inflammation in both preventive and therapeutic schedules. TAT-GILZ accelerated resolution of acute inflammation, reducing the magnitude of PMN infiltration and shortening the resolution interval. Additionally, we showed that TAT-GILZ treatment was associated with decreased levels of the important proinflammatory cytokines, IL-6 and TNF-α. Indeed, in more complex models of inflammation where TAT-GILZ was used it was an effective strategy to control inflammation. For instance, TAT-GILZ administration promoted a protective effect in a model of inflammatory bowel disease (9) and spinal cord injury (12). Moreover, recent studies showed that GILZ overexpression inhibits endothelial cell adhesion function (42) and protects against endotoxemia (43) and arthritis (13).

The apoptosis of neutrophils is an important event in resolution of acute inflammation (2, 15, 21). The involvement of GILZ in the process of apoptosis has been suggested by experiments in GILZ transgenic mice, which overexpress GILZ in the T cell lineage. Thymocytes from these mice undergo apoptosis, activate caspase-8 and caspase-3, and downregulate Bcl-x_L, suggesting that GILZ has effects similar those of GCs (44). Alternatively, another study showed that GILZ inhibited thymocyte apoptosis induced by TCR activation by inhibiting NF-κB activity and IL-10 production (45). Additionally, GILZ did not induce apoptosis in mature mouse T cell lymphocytes (8, 44). These results indicate that GILZ regulates T cell apoptosis and, similar to GC, induces apoptosis in resting T cells while protecting activated T lymphocytes. Inhibition of the PI3K/Akt pathway resulted in GILZ upregulation and increased apoptosis of multiple myeloma cells (46). Interestingly, GILZ acts as a Ras signal suppressor and decreases activation of ERK and Akt, leading to reduction of cell proliferation and transformation (47). Furthermore, GILZ interacts with mammalian target of rapamycin complex 2, inhibiting AKT phosphorylation and activating FOXO3a-mediated transcription of the proapoptotic protein Bim in BCR-ABL^+ cells (48). In our study, we demonstrated, to our knowledge for the first time, that TAT-GILZ was able to induce neutrophil apoptosis and inhibit important prosurvival pathways such as p-ERK1/2, NF-κB, and Mcl-1. Altogether, these data clearly do show that GILZ plays an important role in the signaling events underlying the proapoptotic and proresolving effects that lead to resolution of acute inflammation.

A study of Yang et al. (20) showed that GILZ could be a mediator of the anti-inflammatory effects of AnxA1, a known anti-inflammatory and proresolving protein (4, 32). They showed lower levels of GILZ in Dex-treated AnxA1-deficient macrophages, as compared with Dex-treated WT macrophages (20). A follow-up study using lung fibroblasts showed that the involvement of AnxA1 in GC induction of GILZ was independent of formyl peptide receptor 2, suggesting that there was no requirement for engagement of the AnxA1 receptor for effects on GILZ expression (49). Our group has previously shown that by inhibiting AnxA1, the effect of Dex to induce resolution of neutrophilic inflammation was abolished (15). Importantly, in the present study, we show that this effect is associated with decreased GILZ expression, suggesting that in vivo there is a crosstalk between GILZ and AnxA1. Moreover, the inhibition of the compensatory increase of AnxA1 in $GILZ^{-/-}$ mice induced refractoriness to resolution induced by Dex. Indeed, we were able to show in vivo that injection of the AnxA1 peptide Ac2-26 in LPS-inflamed mice increased GILZ expression in macrophages, an effect not shown in vitro (20). Therefore, these findings suggest a regulatory relationship between AnxA1 and GILZ, in which AnxA1 is involved in a mechanism leading to modulation of GILZ expression in in vivo settings.

In the model of LPS-induced pleurisy used in this study, GILZ deficiency resulted in a reduction of the number of total leukocytes and mononuclear cells, but curiously the absence of GILZ did not modify the natural course of resolution of neutrophilic inflammation, that is, neutrophilic inflammation resolved similarly in GILZ-deficient and WT mice. In a self-resolving model of zymosan-induced peritonitis, AnxA1-deficient mice resolved inflammation similarly to WT mice, despite greater numbers of neutrophils and increased amounts of the chemokines KC and IL-1β at early time points (50). Additionally, AnxA1 KO mice showed defective GC suppression of inflammation in carrageenan-induced edema, zymosan-induced peritonitis, and Ag-induced arthritis, when GC was administered previously to the inflammatory stimulus (18, 32). In the context of GILZ deficiency it has been demonstrated that inhibition of endogenous GILZ by small interfering RNA

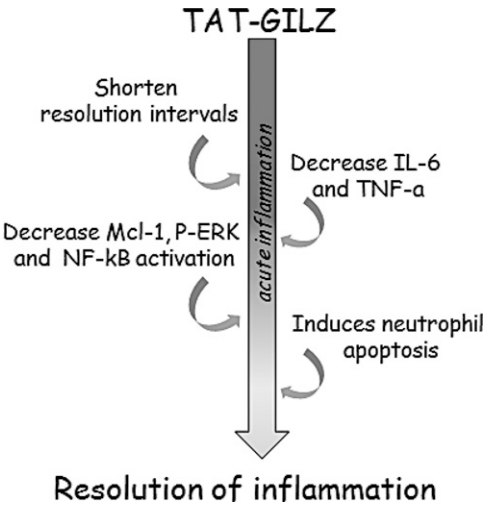

FIGURE 7. Proposed model for TAT-GILZ–induced resolution of inflammation. TAT-GILZ, a GILZ fusion protein containing a TAT peptide to allow the in vivo delivery of the protein, decreases proinflammatory cytokines IL-6 and TNF-α, inhibits prosurvival proteins such as p-ERK1/2, p–IκB-α, and Mcl-1, short resolution intervals, and also promotes neutrophil apoptosis. These sequences of events result in an efficient resolution of acute inflammation.

increased the severity of a mouse model of collagen-induced arthritis, with enhanced production of TNF-α and IL-1β (10). However, GILZ KO mice did not present difference in severity of inflammation as compared with WT mice in a model of arthritis (13), although GILZ treatment using an adenoviral strategy was therapeutically effective. This latter study (13) is in agreement with our findings using LPS-induced inflammation, showing that absence of GILZ does not modify the severity or course of natural resolution of inflammation, but that an exogenous GILZ-based strategy efficiently resolves acute inflammation. Taken together, these studies indicate that GILZ may affect differently the outcome of inflammation resolution in different experimental models, possibly due to the fact that GILZ and AnxA1 influence each other's expression. In contrast to these findings, it has been shown that there was worsening of arthritis and refractoriness to Dex treatment after silencing GILZ expression in vivo (10). In our experiments, the kinetics of cell influx and the effects of Dex were unaltered in GILZ-deficient mice. Because in our experimental conditions there was enhanced expression of AnxA1 in the absence of GILZ, it was reasonable to suggest that compensatory AnxA1 expression in GILZ KO mice could replace the loss of GILZ. Interestingly, increased levels of AnxA1 in GILZ-deficient mice after LPS stimulus were associated with increased plasma levels of corticosterone. More importantly, blockade of AnxA1 with a neutralizing Ab blocked the capacity of GCs to promote resolution in GILZ-deficient mice, suggesting that the increase of AnxA1 in the absence of GILZ could account for the normal resolution phenotype in these mice. The ability of AnxA1 to exert inhibitory effects in the absence of GILZ also likely explains the hitherto perplexing observation that GILZ deficiency does not appear to impair the anti-inflammatory effects of GC (13). In this context, the potential for a GILZ-based therapy to be proresolving during inflammation is fairly clear. There are as yet no data on which to determine whether such an approach would result in GC-like immunosuppressive effects, as well as increased infections, during chronic therapy.

In conclusion, our findings indicate that although endogenous GILZ is redundant for the self-resolving model of acute inflammation used in the present study, therapeutic administration of GILZ efficiently induces a proapoptotic program in neutrophils leading to resolution of acute inflammation (Fig. 7). To our knowledge, this is the first observation that GILZ promotes resolution of neutrophilic inflammation by inducing apoptosis of neutrophils. Moreover, our results suggest that the lack of phenotype of GILZ-deficient mice in some experimental contexts is likely due to compensation mediated by an increase in AnxA1 expression. Hence, these results reinforce the idea that there is a coordinated regulation of GILZ and AnxA1, and that exploitation of the association of these proteins may represent a powerful anti-inflammatory strategy for the treatment of inflammatory diseases.

Acknowledgments

We thank Frankcinéia Assis and Ilma Marçal for technical assistance.

Disclosures

The authors have no financial conflicts of interest.

References

1. Serhan, C. N., S. D. Brain, C. D. Buckley, D. W. Gilroy, C. Haslett, L. A. O'Neill, M. Perretti, A. G. Rossi, and J. L. Wallace. 2007. Resolution of inflammation: state of the art, definitions and terms. *FASEB J.* 21: 325–332.
2. Alessandri, A. L., L. P. Sousa, C. D. Lucas, A. G. Rossi, V. Pinho, and M. M. Teixeira. 2013. Resolution of inflammation: mechanisms and opportunity for drug development. *Pharmacol. Ther.* 139: 189–212.
3. Sousa, L. P., A. L. Alessandri, V. Pinho, and M. M. Teixeira. 2013. Pharmacological strategies to resolve acute inflammation. *Curr. Opin. Pharmacol.* 13: 625–631.
4. Perretti, M., and F. D'Acquisto. 2009. Annexin A1 and glucocorticoids as effectors of the resolution of inflammation. *Nat. Rev. Immunol.* 9: 62–70.
5. Beaulieu, E., and E. F. Morand. 2011. Role of GILZ in immune regulation, glucocorticoid actions and rheumatoid arthritis. *Nat. Rev. Rheumatol.* 7: 340–348.
6. Clark, A. R., and M. G. Belvisi. 2012. Maps and legends: the quest for dissociated ligands of the glucocorticoid receptor. *Pharmacol. Ther.* 134: 54–67.
7. D'Adamio, F., O. Zollo, R. Moraca, E. Ayroldi, S. Bruscoli, A. Bartoli, L. Cannarile, G. Migliorati, and C. Riccardi. 1997. A new dexamethasone-induced gene of the leucine zipper family protects T lymphocytes from TCR/CD3-activated cell death. *Immunity* 7: 803–812.
8. Ayroldi, E., and C. Riccardi. 2009. Glucocorticoid-induced leucine zipper (GILZ): a new important mediator of glucocorticoid action. *FASEB J.* 23: 3649–3658.
9. Cannarile, L., S. Cuzzocrea, L. Santucci, M. Agostini, E. Mazzon, E. Esposito, C. Muià, M. Coppo, R. Di Paola, and C. Riccardi. 2009. Glucocorticoid-induced leucine zipper is protective in Th1-mediated models of colitis. *Gastroenterology* 136: 530–541.
10. Beaulieu, E., D. Ngo, L. Santos, Y. H. Yang, M. Smith, C. Jorgensen, V. Escriou, D. Scherman, G. Courties, F. Apparailly, and E. F. Morand. 2010. Glucocorticoid-induced leucine zipper is an endogenous antiinflammatory mediator in arthritis. *Arthritis Rheum.* 62: 2651–2661.
11. Srinivasan, M., and S. Janardhanam. 2011. Novel p65 binding glucocorticoid-induced leucine zipper peptide suppresses experimental autoimmune encephalomyelitis. *J. Biol. Chem.* 286: 44799–44810.
12. Esposito, E., S. Bruscoli, E. Mazzon, I. Paterniti, M. Coppo, E. Velardi, S. Cuzzocrea, and C. Riccardi. 2012. Glucocorticoid-induced leucine zipper (GILZ) over-expression in T lymphocytes inhibits inflammation and tissue damage in spinal cord injury. *Neurotherapeutics* 9: 210–225.
13. Ngo, D., E. Beaulieu, R. Gu, A. Leaney, L. Santos, H. Fan, Y. Yang, W. Kao, J. Xu, V. Escriou, et al. 2013. Divergent effects of endogenous and exogenous glucocorticoid-induced leucine zipper in animal models of inflammation and arthritis. *Arthritis Rheum.* 65: 1203–1212.
14. Solito, E., A. Kamal, F. Russo-Marie, J. C. Buckingham, S. Marullo, and M. Perretti. 2003. A novel calcium-dependent proapoptotic effect of annexin 1 on human neutrophils. *FASEB J.* 17: 1544–1546.
15. Vago, J. P., C. R. Nogueira, L. P. Tavares, F. M. Soriani, F. Lopes, R. C. Russo, V. Pinho, M. M. Teixeira, and L. P. Sousa. 2012. Annexin A1 modulates natural and glucocorticoid-induced resolution of inflammation by enhancing neutrophil apoptosis. *J. Leukoc. Biol.* 92: 249–258.
16. Maderna, P., S. Yona, M. Perretti, and C. Godson. 2005. Modulation of phagocytosis of apoptotic neutrophils by supernatant from dexamethasone-treated macrophages and annexin-derived peptide Ac2-26. *J. Immunol.* 174: 3727–3733.
17. Dalli, J., C. P. Jones, D. M. Cavalcanti, S. H. Farsky, M. Perretti, and S. M. Rankin. 2012. Annexin A1 regulates neutrophil clearance by macrophages in the mouse bone marrow. *FASEB J.* 26: 387–396.
18. Hannon, R., J. D. Croxtall, S. J. Getting, F. Roviezzo, S. Yona, M. J. Paul-Clark, F. N. Gavins, M. Perretti, J. F. Morris, J. C. Buckingham, and R. J. Flower. 2003. Aberrant inflammation and resistance to glucocorticoids in annexin $1^{-/-}$ mouse. *FASEB J.* 17: 253–255.
19. Montero-Melendez, T., J. Dalli, and M. Perretti. 2013. Gene expression signature-based approach identifies a pro-resolving mechanism of action for histone deacetylase inhibitors. *Cell Death Differ.* 20: 567–575.
20. Yang, Y. H., D. Aeberli, A. Dacumos, J. R. Xue, and E. F. Morand. 2009. Annexin-1 regulates macrophage IL-6 and TNF via glucocorticoid-induced leucine zipper. *J. Immunol.* 183: 1435–1445.
21. Sousa, L. P., F. Lopes, D. M. Silva, L. P. Tavares, A. T. Vieira, B. M. Rezende, A. F. Carmo, R. C. Russo, C. C. Garcia, C. A. Bonjardim, et al. 2010. PDE4 inhibition drives resolution of neutrophilic inflammation by inducing apoptosis in a PKA-PI3K/Akt-dependent and NF-κB-independent manner. *J. Leukoc. Biol.* 87: 895–904.
22. Souza, D. G., C. T. Fagundes, F. A. Amaral, D. Cisalpino, L. P. Sousa, A. T. Vieira, V. Pinho, J. R. Nicoli, L. Q. Vieira, I. M. Fierro, and M. M. Teixeira. 2007. The required role of endogenously produced lipoxin A_4 and annexin-1 for the production of IL-10 and inflammatory hyporesponsiveness in mice. *J. Immunol.* 179: 8533–8543.
23. Bannenberg, G. L., N. Chiang, A. Ariel, M. Arita, E. Tjonahen, K. H. Gotlinger, S. Hong, and C. N. Serhan. 2005. Molecular circuits of resolution: formation and actions of resolvins and protectins. *J. Immunol.* 174: 4345–4355.
24. Chiang, N., M. Shinohara, J. Dalli, V. Mirakaj, M. Kibi, A. M. Choi, and C. N. Serhan. 2013. Inhaled carbon monoxide accelerates resolution of inflammation via unique proresolving mediator-heme oxygenase-1 circuits. *J. Immunol.* 190: 6378–6388.
25. Sousa, L. P., A. F. Carmo, B. M. Rezende, F. Lopes, D. M. Silva, A. L. Alessandri, C. A. Bonjardim, A. G. Rossi, M. M. Teixeira, and V. Pinho. 2009. Cyclic AMP enhances resolution of allergic pleurisy by promoting inflammatory cell apoptosis via inhibition of PI3K/Akt and NF-κB. *Biochem. Pharmacol.* 78: 396–405.
26. De Sousa, L. P., B. S. Brasil, B. M. Silva, M. H. Freitas, S. V. Nogueira, P. C. Ferreira, E. G. Kroon, and C. A. Bonjardim. 2005. Plasminogen/plasmin regulates *c-fos* and *egr*-1 expression via the MEK/ERK pathway. *Biochem. Biophys. Res. Commun.* 329: 237–245.
27. Lichtnekert, J., T. Kawakami, W. C. Parks, and J. S. Duffield. 2013. Changes in macrophage phenotype as the immune response evolves. *Curr. Opin. Pharmacol.* 13: 555–564.

28. Schif-Zuck, S., N. Gross, S. Assi, R. Rostoker, C. N. Serhan, and A. Ariel. 2011. Saturated-efferocytosis generates pro-resolving CD11b low macrophages: modulation by resolvins and glucocorticoids. *Eur. J. Immunol.* 41: 366–379.
29. Ariel, A., and C. N. Serhan. 2012. New lives given by cell death: macrophage differentiation following their encounter with apoptotic leukocytes during the resolution of inflammation. *Front. Immunol.* 3: 4.
30. Morris, J. F., S. Omer, E. Davies, E. Wang, C. John, T. Afzal, S. Wain, J. C. Buckingham, R. J. Flower, and H. C. Christian. 2006. Lack of annexin 1 results in an increase in corticotroph number in male but not female mice. *J. Neuroendocrinol.* 18: 835–846.
31. Akasheh, R. T., M. Pini, J. Pang, and G. Fantuzzi. 2013. Increased adiposity in annexin A1-deficient mice. *PLoS ONE* 8: e82608.
32. Yang, Y. H., E. Morand, and M. Leech. 2013. Annexin A1: potential for glucocorticoid sparing in RA. *Nat. Rev. Rheumatol.* 9: 595–603.
33. Hoppstädter, J., B. Diesel, L. K. Eifler, T. Schmid, B. Brüne, and A. K. Kiemer. 2012. Glucocorticoid-induced leucine zipper is downregulated in human alveolar macrophages upon Toll-like receptor activation. *Eur. J. Immunol.* 42: 1282–1293.
34. Hahn, R. T., J. Hoppstädter, K. Hirschfelder, N. Hachenthal, B. Diesel, S. M. Kessler, H. Huwer, and A. K. Kiemer. 2014. Downregulation of the glucocorticoid-induced leucine zipper (GILZ) promotes vascular inflammation. *Atherosclerosis* 234: 391–400.
35. Soehnlein, O., and L. Lindbom. 2010. Phagocyte partnership during the onset and resolution of inflammation. *Nat. Rev. Immunol.* 10: 427–439.
36. Bystrom, J., I. Evans, J. Newson, M. Stables, I. Toor, N. van Rooijen, M. Crawford, P. Colville-Nash, S. Farrow, and D. W. Gilroy. 2008. Resolution-phase macrophages possess a unique inflammatory phenotype that is controlled by cAMP. *Blood* 112: 4117–4127.
37. Stables, M. J., S. Shah, E. B. Camon, R. C. Lovering, J. Newson, J. Bystrom, S. Farrow, and D. W. Gilroy. 2011. Transcriptomic analyses of murine resolution-phase macrophages. *Blood* 118: e192–e208.
38. Dalli, J., and C. N. Serhan. 2012. Specific lipid mediator signatures of human phagocytes: microparticles stimulate macrophage efferocytosis and pro-resolving mediators. *Blood* 120: e60–e72.
39. Berrebi, D., S. Bruscoli, N. Cohen, A. Foussat, G. Migliorati, L. Bouchet-Delbos, M. C. Maillot, A. Portier, J. Couderc, P. Galanaud, et al. 2003. Synthesis of glucocorticoid-induced leucine zipper (GILZ) by macrophages: an anti-inflammatory and immunosuppressive mechanism shared by glucocorticoids and IL-10. *Blood* 101: 729–738.
40. Scannell, M., M. B. Flanagan, A. deStefani, K. J. Wynne, G. Cagney, C. Godson, and P. Maderna. 2007. Annexin-1 and peptide derivatives are released by apoptotic cells and stimulate phagocytosis of apoptotic neutrophils by macrophages. *J. Immunol.* 178: 4595–4605.
41. Bereshchenko, O., M. Coppo, S. Bruscoli, M. Biagioli, M. Cimino, T. Frammartino, D. Sorcini, A. Venanzi, M. Di Sante, and C. Riccardi. 2014. GILZ promotes production of peripherally induced Treg cells and mediates the crosstalk between glucocorticoids and TGF-β signaling. *Cell Rep.* 7: 464–475.
42. Cheng, Q., H. Fan, D. Ngo, E. Beaulieu, P. Leung, C. Y. Lo, R. Burgess, Y. G. van der Zwan, S. J. White, L. M. Khachigian, et al. 2013. GILZ overexpression inhibits endothelial cell adhesive function through regulation of NF-κB and MAPK activity. *J. Immunol.* 191: 424–433.
43. Pinheiro, I., L. Dejager, I. Petta, S. Vandevyver, L. Puimège, T. Mahieu, M. Ballegeer, F. Van Hauwermeiren, C. Riccardi, M. Vuylsteke, and C. Libert. 2013. LPS resistance of SPRET/Ei mice is mediated by Gilz, encoded by the *Tsc22d3* gene on the X chromosome. *EMBO Mol. Med.* 5: 456–470.
44. Delfino, D. V., M. Agostini, S. Spinicelli, P. Vito, and C. Riccardi. 2004. Decrease of Bcl-x_L and augmentation of thymocyte apoptosis in GILZ overexpressing transgenic mice. *Blood* 104: 4134–4141.
45. Delfino, D. V., M. Agostini, S. Spinicelli, C. Vacca, and C. Riccardi. 2006. Inhibited cell death, NF-κB activity and increased IL-10 in TCR-triggered thymocytes of transgenic mice overexpressing the glucocorticoid-induced protein GILZ. *Int. Immunopharmacol.* 6: 1126–1134.
46. Grugan, K. D., C. Ma, S. Singhal, N. L. Krett, and S. T. Rosen. 2008. Dual regulation of glucocorticoid-induced leucine zipper (GILZ) by the glucocorticoid receptor and the PI3-kinase/AKT pathways in multiple myeloma. *J. Steroid Biochem. Mol. Biol.* 110: 244–254.
47. Ayroldi, E., O. Zollo, A. Bastianelli, C. Marchetti, M. Agostini, R. Di Virgilio, and C. Riccardi. 2007. GILZ mediates the antiproliferative activity of glucocorticoids by negative regulation of Ras signaling. *J. Clin. Invest.* 117: 1605–1615.
48. Joha, S., A. L. Nugues, D. Hétuin, C. Berthon, X. Dezitter, V. Dauphin, F. X. Mahon, C. Roche-Lestienne, C. Preudhomme, B. Quesnel, and T. Idziorek. 2012. GILZ inhibits the mTORC2/AKT pathway in BCR-ABL$^+$ cells. *Oncogene* 31: 1419–1430.
49. Jia, Y., E. F. Morand, W. Song, Q. Cheng, A. Stewart, and Y. H. Yang. 2013. Regulation of lung fibroblast activation by annexin A1. *J. Cell. Physiol.* 228: 476–484.
50. Damazo, A. S., S. Yona, R. J. Flower, M. Perretti, and S. M. Oliani. 2006. Spatial and temporal profiles for anti-inflammatory gene expression in leukocytes during a resolving model of peritonitis. *J. Immunol.* 176: 4410–4418.